International Research Journal of Engineering and Technology (IRJET) e-ISSN: 2395-0056
Volume: 02 Issue: 06 | Sep-2015 www.irjet.net p-ISSN: 2395-0072

SORET AND DUFOUR EFFECTS ON MHD MIXED CONVECTION STAGNATION POINT FLOW OF A RADIATING AND CHEMICALLY REACTING FLUID PAST AN ISOTHERMAL VERTICAL PLATE IN POROUS MEDIUM WITH VISCOUS DISSIPATION AND HEAT GENERATION/ ABSORPTION

S. Suneetha[1*], E. Manjoolatha[2] M. Prasanna Lakshmi[3]

[1]Assistant Professor, Dept of Applied Mathematics, Yogi Vemana University, Kadapa Dist.,A.P., India
[2]Assistant Professor, Dept of Mathematics, Sri Annamacharya Institute of Technology & Sciences, Tirupati, A.P., India.
[3]Lecturer, Dept of Mathematics, Sri Vignana Deepthi Degree College, Chittoor, A.P., India.

Abstract - *This paper analyses the Soret and Dufour effects on hydro magnetic mixed convection stagnation point flow of a radiating and chemically reacting fluid past an isothermal vertical plate with heat generation/absorption by taking viscous dissipation into account. The governing boundary layer equations have been transformed to a two-point boundary value problem in similarity variables and the resultant problem is solved numerically using the Runge-Kutta fourth order technique along with shooting method. The effects of various governing parameters on the fluid velocity, temperature, concentration, skin-friction coefficient, Nusselt number and Sherwood number are shown in figures and tables and analyzed in detail.*

Key Words: *MHD, Soret and Dufour effects, Viscous Dissipation, Radiation, heat generation/absorption and Chemical reaction*

1. INTRODUCTION

Convective heat transfer in porous media has been a subject of great interest for the last several decades. The research activities in this field has been accelerated because of a broad range of applications in various disciplines, such as geophysical, thermal and insulating engineering, modeling of packed sphere beds, solar power collector, pollutant dispersion in aquifers, cooling of electronic systems, ventilation of rooms, crystal growth in liquids, chemical catalytic reactors, grain storage devices, petroleum reservoirs, ground hydrology, fiber and granular insulation, nuclear waste repositories, high-performance building insulation, post accident heat removal from pebble-bed nuclear reactors, concepts of aerodynamics heat shielding with transpiration cooling, etc.[1-5]. In fluid dynamics, a stagnation point is a point in a flow field where the local velocity of the fluid is zero. Stagnation points exist at the surface of objects in the flow field, where the fluid is brought to rest by the object. A stagnation point occurs whenever a flow impinges on a solid object. Usually there are other important features of the flow.

Singh et al. [6], investigated the effect of volumetric heat generation/absorption on mixed convection stagnation point flow on an isothermal vertical plate in porous media. The volumetric rate of heat generation Q [Watt/m3] in the boundary layer flows generally has been presented in the literature (see, [7, 8, 9]). Shateyi et al. [10], examined the effects of thermal radiation, hall currents, Soret, and Dufour on MHD flow by mixed convection over a vertical surface in porous media. It is worth also mentioning that radiation effects on the convective flow are important in the context of space technology and process involving high temperatures.

Pop [11] investigated the effects of radiation on mixed convection flow over a vertical pin, whereas Mohammedein and El-Amin [12] studied the problem of thermal dispersion and radiation effects on non-Darcy natural convection in a fluid saturated porous medium. Thermal radiation heat transfer effects on the Rayleigh of gray viscous fluids under the effect of a transverse magnetic field have been investigated by Duwairi and Duwairi [13]. Pop et al. [14] investigated the steady two-dimensional stagnation-point flow of an incompressible fluid over a stretching sheet by taking into account radiation effects using the Rosseland approximation to model the heat transfer. Hayat et al [15] studied heat and mass transfer for Soret and Dufour effect on mixed convection boundary layer flow over a stretching vertical

surface in a porous medium filled with a visco-elastic fluid. [16], investigated mixed convection in the stagnation-point flow of a Maxwell fluid towards a vertical stretching surface.

Gebhart and Mollendorf [17] considered the effects of viscous dissipation for external natural convection flow over a surface. Soundalgekar [18] analyzed viscous dissipative heat on the two-dimensional unsteady free convective flow past an infinite vertical porous plate when the temperature oscillates in time and there is constant suction at the plate. Israel Cookey et al. [19] investigated the influence of viscous dissipation and radiation on unsteady MHD free convection flow past an infinite heated vertical plate in a porous medium with time dependent suction. Ramachandra Prasad and Bhaskar Reddy [20]studied radiation and mass transfer effects on an unsteady MHD free convection flow past a heated vertical plate in a porous medium. Gnaneshwara Reddy and Bhaskar Reddy [21] studied radiation and mass transfer effects on an unsteady MHD free convection flow past a heated vertical porous plate with viscous dissipation. Radiation and darcy effects on unsteady MHD heat and mass transfer flow of a chemically reacting fluid past an impulsively started vertical plate with heat generation was reported by Suneetha and Bhaskar Reddy [22].

The aim of the present chapter is to analyze the effects of Soret, Dufour, chemical reaction and volumetric heat generation/absorption on mixed convection stagnation point flow of a viscous incompressible electrically conducting and radiating fluid past an isothermal vertical plate in a porous medium by taking viscous dissipation into account. The governing boundary layer equations have been transformed to a two-point boundary value problem in similarity variables and the resultant problem is solved numerically using the Runge-Kutta method with shooting technique. The effects of various governing parameters on the fluid velocity, temperature, concentration, skin-friction coefficient, Nusselt number and Sherwood number are shown in figures and tables and analyzed in detail.

1. MATHEMATICAL ANALYSIS

A steady two-dimensional laminar mixed convection flow of a viscous incompressible electrically conducting, radiating and chemically reacting fluid along a vertical isothermal plate embedded in fluid saturated porous medium, in the presence of volumetric rate of heat generation and viscous dissipation, is considered. The fluid is assumed to be gray, absorbing-emitting but non-scattering. A uniform magnetic field is applied in the direction perpendicular to the plate. The transverse applied magnetic field and magnetic Reynolds number are assumed to be very small, so that the induced magnetic field and Hall effects are negligible. The x-axis is taken along the plate and y-axis is normal to the plate and the flow is confined in half plane y > 0. The potential flow arrives from the y-axis and impinges on plate, which divides at stagnation point into two streams and the viscous flow adheres to the plate. The velocity distribution in the potential flow is given by $U_\infty = cx$ and $V_\infty = cy$, where c is a positive constant. Following Singh et al. [6] the linear Darcy term representing distributed body force due to porous media is retained while the non-linear Forchheimer term is neglected. Then, under the usual Boussinesq's approximation, the governing equations of continuity, momentum, energy and species are

Continuity equation

$$\frac{\partial u}{\partial x}+\frac{\partial v}{\partial y}=0 \qquad (2.1)$$

Momentum equation

$$u\frac{\partial u}{\partial x}+v\frac{\partial u}{\partial y}=\upsilon\frac{\partial^2 u}{\partial y^2}-\frac{\sigma B_0^2}{\rho}(u-U_\infty)+g\beta_T(T-T_\infty)+g\beta_C(C-C_\infty)-\frac{\upsilon}{\bar{K}}(u-U_\infty)+U_\infty\frac{dU_\infty}{dx} \qquad (2.2)$$

Energy equation

$$u\frac{\partial T}{\partial x}+v\frac{\partial T}{\partial y}=\alpha\frac{\partial^2 T}{\partial y^2}-\frac{\alpha}{k}\frac{\partial q_r}{\partial y}+\frac{\upsilon}{\rho c_p}\left(\frac{\partial u}{\partial y}\right)^2+Q(T-T_\infty)+\frac{D_e k_T}{c_s c_p}\frac{\partial^2 C}{\partial y^2} \qquad (2.3)$$

Species equation

$$u\frac{\partial C}{\partial x}+v\frac{\partial C}{\partial y}=D_e\frac{\partial^2 C}{\partial y^2}+\frac{D_e k_T}{T_m}\frac{\partial^2 T}{\partial y^2}-k_0(C-C_\infty)^n \qquad (2.4)$$

The boundary conditions for the velocity, temperature and concentration fields are

$$u=0, v=0, T=T_w, C=C_w \quad \text{at} \quad y=0$$
$$u\to U_\infty=cx, T\to T_\infty, C\to C_\infty \quad \text{as} \quad y\to\infty \qquad (2.5)$$

where u and v are the velocity components in the x- and y-directions, respectively, ρ is the fluid density, υ is the kinematic viscosity, σ is the electrical conductivity of the fluid, $\bar{K}$ is the permeability of the porous medium, *g* is the gravitational acceleration, β_T is the thermal expansion coefficient, β_C is the coefficient of expansion with concentration, *T* is the temperature, c_p is the specific heat capacity at constant pressure of the fluid, *k* is the thermal conductivity of the fluid, α is the thermal diffusivity of the fluid, q_r is the radiative heat flux, T_w is the

temperature of the plate, Q is the volumetric rate heat generation/absorption, B_0 is the magnetic field of constant strength, D_e is the coefficient of mass diffusivity, c_s is the concentration susceptibility, k_0 is the rate of chemical reaction and n is the order of reaction, respectively.

The radiative heat flux q_r is described by Rosseland approximation such that

$$q_r = -\frac{4\sigma^*}{3K'}\frac{\partial T^4}{\partial y} \tag{2.6}$$

where σ^* and K' are the Stefan-Boltzmann constant and the mean absorption coefficient, respectively.

It should be noted that, by using the Rosseland approximation, the present analysis is limited to optically thick fluids. If the temperature differences within the flow are sufficiently small, then equation (2.6) can be linearized by expanding T^4 into the Taylor's series about T_∞, and neglecting higher order terms, we get

$$T^4 \cong 4T_\infty^3 T - 3T_\infty^4 . \tag{2.7}$$

Using equations (2.7) and (2.8) in equation (2.3), we obtain

$$u\frac{\partial T}{\partial x} + v\frac{\partial T}{\partial y} = \alpha\left(1+\frac{16\sigma^* T_\infty^3}{3K'k}\right)\frac{\partial^2 T}{\partial y^2} + \frac{\upsilon}{\rho c_p}\left(\frac{\partial u}{\partial y}\right)^2 + Q(T-T_\infty) + \frac{D_e k_T}{c_s c_p}\frac{\partial^2 C}{\partial y^2} \tag{2.8}$$

The continuity equation (2.1) is satisfied by the Cauchy Riemann equations

$$u = \frac{\partial \psi}{\partial x} \quad \text{and} \quad v = -\frac{\partial \psi}{\partial y}$$

where $\psi(x, y)$ is the stream function.

In order to transform equations (2.2) and (2.3) into a set of ordinary differential equations, the following similarity transformations and dimensionless variables are introduced.

$$\psi(x,y) = \sqrt{c\upsilon x}\, f(\eta), \qquad \eta = y\sqrt{\frac{c}{\upsilon}}, \qquad \theta(\eta) = \frac{T-T_\infty}{T_w - T_\infty},$$

$$\phi(\eta) = \frac{C-C_\infty}{C_w - C_\infty}, M = \frac{\sigma B_0^2}{\rho c}, \qquad Gr = \frac{g\beta_T (T_w - T_\infty)}{U_\infty c},$$

$$Gc = \frac{g\beta_C (C_w - C_\infty)}{U_\infty c}, \quad \Pr = \frac{\upsilon}{\alpha}, \quad Sr = \frac{D_e k_T (T_w - T_\infty)}{\upsilon T_m (C_w - C_\infty)},$$

$$Df = \frac{D_e k_T (C_w - C_\infty)}{\upsilon c_s c_p (T_w - T_\infty)}, \qquad Ec = \frac{U_\infty}{c_p (T_w - T_\infty)},$$

$$Sc = \frac{\upsilon}{D_e}, Ra = \frac{4\sigma^* T_\omega^{\ 3}}{K'k}. \tag{2.9}$$

where $f(\eta)$ is the dimensionless stream function, θ - dimensionless temperature, ϕ - dimensionless concentration, η - similarity variable, M - the magnetic parameter, Gr - the local thermal Grashof number, Gc - the local solutal Grashof number, Ra- radiation parameter, $\Pr$ - the Prandtl number, Sr - the Soret number, Df - the Dufour number, Ec - the Eckert number and Sc - the Schmidt number.

In view of equations (2.6) and (2.9), the equations (2.2), (2.3), and (2.4) transform into

$$f''' + ff'' - f'^2 + Gr\theta + Gc\phi - (K+M)(f'-1) + 1 = 0 \tag{2.10}$$

$$\left(1+\frac{4}{3}Ra\right)\theta'' + \Pr\, f\theta' + Ec\,\Pr\, f''^2 + S\phi + PrDf\,\phi'' = 0 \tag{2.11}$$

$$\phi'' + Scf\theta' + ScSr\theta'' - Sc\gamma\phi^n = 0 \tag{2.12}$$

The corresponding boundary conditions are

$$f = 0,\ f' = 0,\ \theta = 1,\ \phi(0) = 1 \qquad \text{at} \qquad \eta = 0$$

$$f' = 1,\ \theta = \phi = 0. \qquad \text{as} \qquad \eta \to \infty \tag{2.13}$$

where the primes denote differentiation with respect to η

Other physical quantities of interest of the problems of this type are the plate surface temperature, the local skin-friction coefficient, the local Nusselt number and Sherwood number, which are proportional to $\theta(0)$, $f''(0)$, $-\theta'(0)$ *and* $-\phi'(0)$ respectively, and are computed numerically and presented in a tabular form.

2. SOLUTION OF THE PROBLEM

The set of coupled non-linear governing boundary layer equations (2.10) - (2.12) together with the boundary conditions (2.13) are solved numerically by using Runge-Kutta fourth order technique along with shooting method.

First of all, higher order non-linear differential Equations (2.10) - (2.12) are converted into simultaneous linear differential equations of first order and they are further transformed into initial value problem by applying the shooting technique (Jain *et al.*[]). The resultant initial value problem is solved by employing Runge-Kutta fourth order technique. The step size $\Delta\eta$ =0.05 is used to obtain the numerical solution with five decimal place accuracy as the criterion of convergence. From the process of numerical computation, the skin-friction coefficient, the Nusselt number and the Sherwood number, which are respectively proportional to $f''(0), -\theta'(0)$ and $-\phi'(0)$, are also sorted out and their numerical values are presented in a tabular form.

3. RESULTS AND DISCUSSION

The governing equations (2.10) - (2.12) subject to the boundary conditions (2.13) are integrated as described in section 3. In order to get a clear insight of the physical problem, the velocity, temperature and concentration have been discussed by assigning numerical values to the parameters encountered in the problem. The effects of various parameters on velocity profiles in the boundary layer are depicted in Figs. 1-7. The effects of various parameters on temperature in the boundary layer are depicted in Figs. 8-14. The effects of various parameters on concentration in the boundary layer are depicted in Figs. 15-22.

Fig. 1 shows the dimensionless velocity profiles for different values of magnetic parameter (*M).* It is seen that, as expected, the velocity decreases with an increase of magnetic parameter (*M)*. The magnetic parameter is found to retard the velocity at all points of the flow field. It is because that the application of transverse magnetic field will result in a resistive type force (Lorentz force) similar to drag force which tends to resist the fluid flow and thus reducing its velocity. Also, the boundary layer thickness decreases with an increase in the magnetic parameter. Fig.2 illustrates the effect of the thermal Grashof number (*Gr*) on the velocity field. The thermal Grashof number signifies the relative effect of the thermal buoyancy force to the viscous hydrodynamic force. The flow is accelerated due to the enhancement in buoyancy force corresponding to an increase in the thermal Grashof number i.e. free convection effects. It is noticed that the thermal Grashof number (*Gr*) influences the velocity within the boundary layer when compared to far away from the plate. It is seen that as the thermal Grashof number (*Gr*) increases, the velocity increases.

The effect of mass (solutal) Grashof number (*Gc*) on the velocity is illustrated in Fig.3. The mass (solutal) Grashof number (*Gc*) defines the ratio of the species buoyancy force to the viscous hydrodynamic force. It is noticed that the velocity increases with increasing values of the solutal Grashof number. Further as the mass Grashof number (*Gc*) increases, the velocity field near the boundary layer increases. It is noticed that, for higher values of mass Grashof number (*Gc*), the profiles are found to be more parabolic. Fig.4 illustrates the effect of Eckert number (*Ec*) on the velocity. It is noticed that as the Eckert number (*Ec*) increases, the velocity decreases. As seen in the earlier cases, far away from the plate, the effect is not that much significant.

Fig. 5 shows the variation of the velocity boundary-layer with the Dufour number (D_f). It is noticed that the velocity boundary layer thickness increases with an increase in the Dufour number. Fig. 6 depicts the variation of the velocity boundary-layer with the Soret number (*Sr)*. It is noticed that the velocity boundary layer thickness decreases with an increase in the Soret number. The effect of the chemical reaction parameter γ on the velocity is illustrated in Fig.7. It is observed that as the chemical reaction parameter increases, the velocity boundary layer thickness decreases.

The effect of the magnetic parameter (*M*) on the temperature is illustrated in Fig.8. It is observed that as the magnetic parameter (*M*) increases, the temperature increases. From Figs. 9 and 10, it is observed that the thermal boundary layer thickness decreases with an increase in thermal or Solutal Grashof number (*Gr* or *Gc*). Fig. 11 illustrates the effect of Eckert number (Ec) on the temperature. It is noticed that as the Eckert number (Ec) increases an increasing trend in the temperature field is noticed.

Fig.12 illustrates the effect of the Dufour number (D_f) on the temperature. It is noticed that as the Dufour number increases, the temperature increases. Fig. 13 shows the variation of the thermal boundary-layer with the radiation parameter (*Ra*). It is observed that the thermal boundary layer thickness decreases with an increase in the radiation parameter. Fig. 14 shows the variation of the thermal boundary-layer with the heat generation/absorption parameter (*S*). It is noticed that the thermal boundary layer thickness increases with an increase in the heat generation/absorption parameter.

The effect of magnetic parameter (*M)* on the concentration field is illustrated Fig.15. As the magnetic parameter (*M)* increases the concentration is found to be increasing. The effect of buoyancy parameters (Gr,Gc) on the concentration field is illustrated Figs. 16 and 17. It is noticed that the concentration boundary layer thickness decreases with an increase in the thermal or Solutal Grashof number (*Gr* or *Gc*). Fig. 18 illustrates the effect of Eckert number *Ec* on the concentration. As the Eckert number increases, a decreasing trend in the concentration

field is noticed. The influence of the Dufour number (D_f) on the concentration field is shown in Fig.19. It is noticed that the concentration decreases monotonically with the increase of the Dufour number. The influence of the Soret number (*Sr)* on the concentration field is shown in Fig.20. It is noticed that the concentration increases monotonically with the increase of the Soret number. Fig. 21 shows the variation of the concentration boundary-layer with the radiation parameter (*Ra)*. It is observed that the concentration boundary layer thickness decreases with an increase in the Radiation parameter. Fig. 22 shows the variation of the concentration boundary-layer with the chemical reaction parameter (γ). It is seen that the concentration boundary layer thickness decreases with an increase in the chemical reaction parameter.

Table 1 presents the variations of the skin friction coefficient, Nusselt number and the Sherwood number for different values of the governing parameters of the flow model. Here, the values of Dufour number and Soret number are chosen so that their product is constant provided that the mean temperature is also kept constant. It is clearly seen that the skin-friction increases with an increase in the parameter *M* or *S* or *Gr* or *Gc* or *K* or *Pr* or *Sc* or *n*, whereas it decreases as *Ra* or *Df* or *Sr* or *Ec* or γ increases. Similarly, the Nusselt number coefficient increases at the plate, when *Gr* or *Gc* or *Df* or *Sr* or *Ra* or *Ec* or γ increases, while it decreases when the parameters *S* or *K* or *Pr* or *Sc* or *M* or *n* increases. It is interesting to note that Sherwood number at the plate increases with an increase in *Gr* or *Ra* or *Ec* or *Df* or *Sr* or γ, whereas it decreases with an increase of the other parameters embedded in the flow model.

In Table 2, the present results are compared with those of Olanrewaju and Gbadeyan [23] and found that there is a perfect agreement.

4. CONCLUSIONS

In the present chapter, the effects of Soret, Dufour, chemical reaction and volumetric heat generation/absorption on mixed convection stagnation point flow of a viscous incompressible electrically conducting and radiating fluid past an isothermal vertical plate in a porous medium by taking viscous dissipation into account, are analyzed. The present analysis revealed that both the temperature and concentration profiles are appreciably influenced by the Dufour and Soret effects. Therefore, we can conclude that for fluids with medium molecular weight (*H2*, air), Dufour and Soret effects should not be neglected. Radiation, chemical reaction, and magnetic strength parameters have greater influence on the fluid velocity, temperature, and concentration boundary layer thicknesses. As the Eckert number (Ec) increases, the rate of heat transfer and the rate of mass transfer increase, while the skin-friction decreases. Also, as the Eckert number (Ec) increases, the fluid temperature and velocity increase, while the concentration decreases. It is interesting to note that the skin-friction and the rate of mass transfer increase, while the rate of heat transfer decreases with the increase in the heat generation/absorption parameter (S). Also, the fluid temperature and velocity increase with an increase in the heat generation/absorption parameter (S). Finally, the order of the reaction has little influence on the concentration boundary layer thickness.

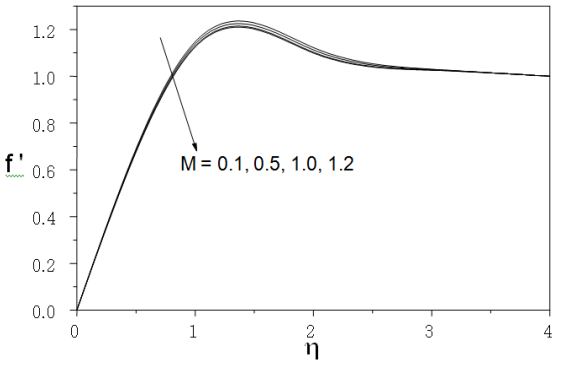

Fig.1: Variation of the velocity f' with *M* for Pr=0.72, Sc=0.24, Gr=Gc=K=Ec=Ra=0.1, n=1, S=0, Sr=2, Df=0.03, γ =1

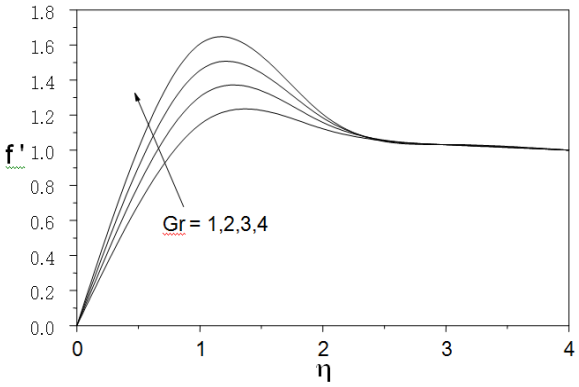

Fig.2: Variation of the velocity f' with *Gr* for Pr=0.72, Sc=0.24, n=1, Gc=M=K=Ec=Ra=0.1, S=0, Sr=2, Df=0.03, γ =1.

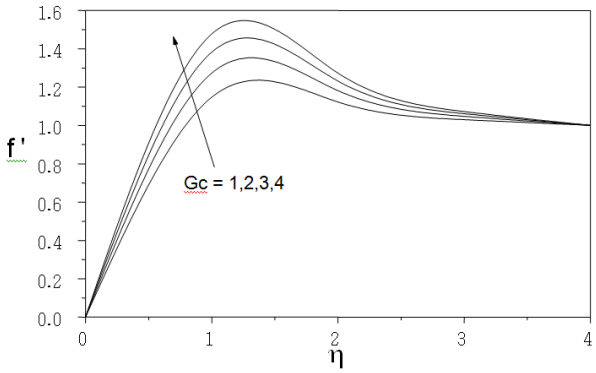

Fig.3: Variation of the velocity f' with *Gc*
For Pr=0.72, Sc=0.24,Gr=M=K=Ra=Ec=0.1, S=0, Sr=2,n=1, Df=0.03, γ =1.

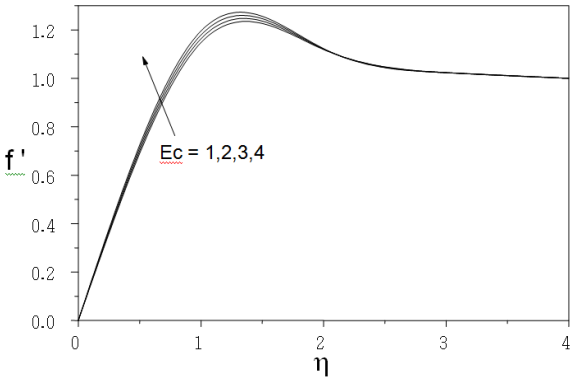

Fig.4: Variation of the velocity f' with *Ec*
for Pr=0.72, Sc=0.24, Gr=Gc=M=Ra=K=0.1, n=1, S=0, Sr=2, Df=0.03, γ =1.

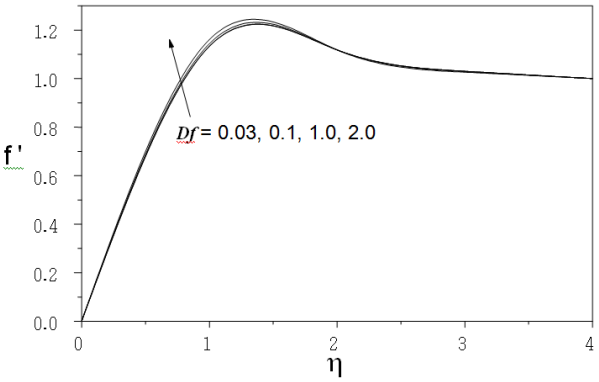

Fig.5: Variation of the velocity f' with *Df*
for Pr=0.72, Sc=0.24, Gr=Gc=M=K=Ra=Ec=0.1, S=0, Sr=2, n=1, γ =1.

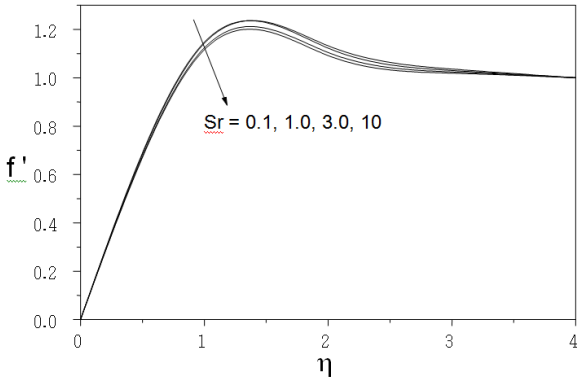

Fig.6: Variation of the velocity f' with *Sr*
for Pr=0.72, Sc=0.24, Gr=Gc=M=Ra=K=Ec=0.1, S=0, n=1, Df=0.03, γ =1.

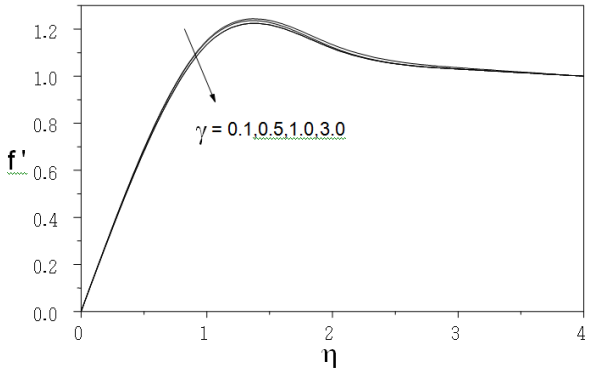

Fig.7: Variation of the velocity f' with γ
for Pr=0.72, Sc=0.24, Gr=Gc=M=K=Ra=Ec=0.1, S=0, Sr=2, Df=0.03, n=1.

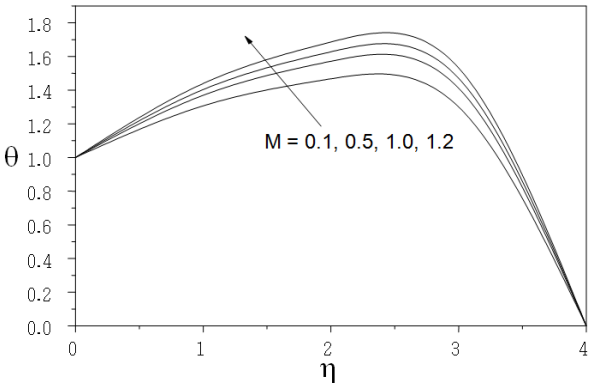

Fig.8: Variation of the temperature θ with *M*
for Pr=0.72, Sc=0.24, Gr=Gc=K=Ec=Ra=0.1, S=0, Sr=2, Df=0.03, n= γ =1.

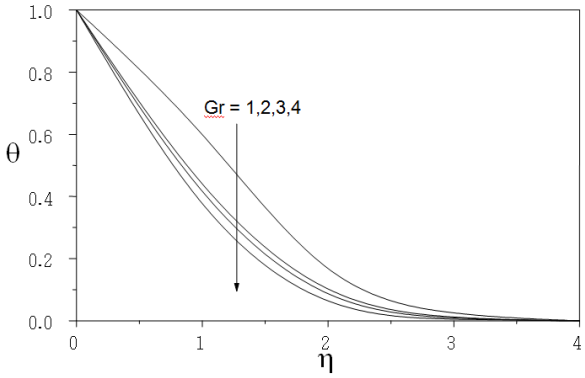

Fig.9: Variation of the temperature θ with *Gr* for Pr=0.72, Sc=0.24, Gc=M=K=Ec=Ra=0.1, S=0, Sr=2, Df=0.03, n= γ =1

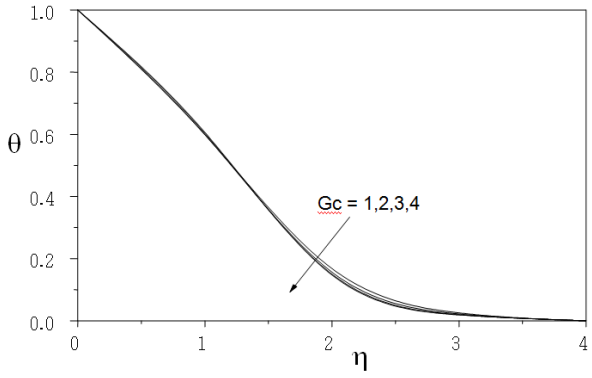

Fig.10: Variation of the temperature θ with Gc for Pr=0.72, Sc=0.24, Gr=M=K=Ra=Ec=0.1, S=0, Sr=2, Df=0.03, n= γ =1.

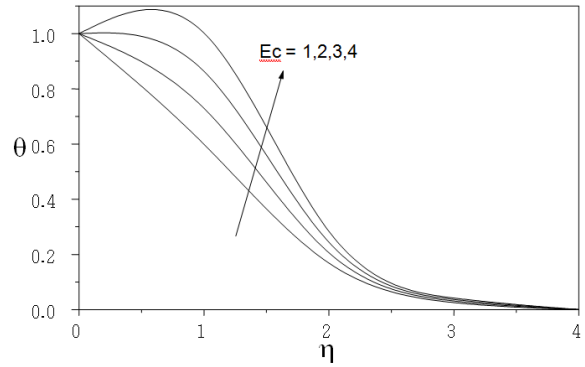

Fig.11: Variation of the temperature θ with *Ec* for Pr=0.72, Sc=0.24, Gr=Gc=Ra=M=K=0.1, S=0, Sr=2, Df=0.03, n= γ =1.

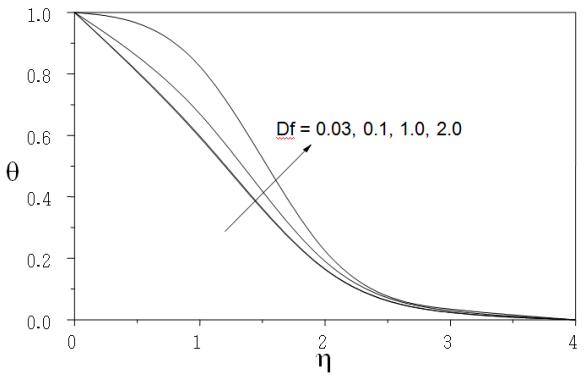

Fig.12: Variation of the temperature θ with Df for Pr=0.72, Sc=0.24, Gr=Gc=Ra=M=K=0.1, S=0, Sr=2, n= γ =1.

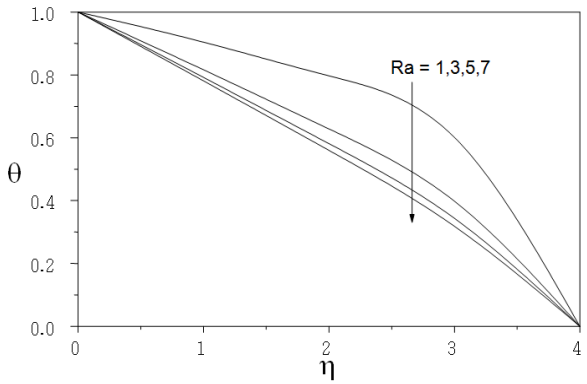

Fig.13: Variation of the temperature θ with *Ra* for Pr=0.72, Sc=0.24, Gr=Gc=M=K=0.1, S=0, Sr=2, Df=0.03, n= γ =1.

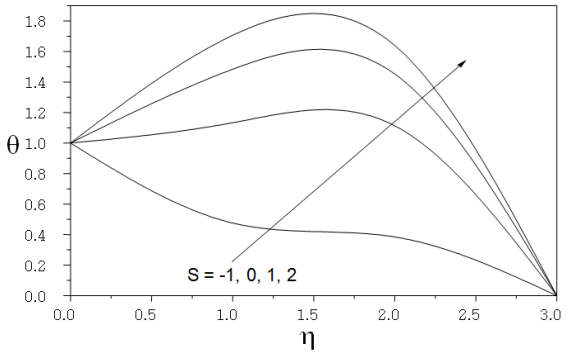

Fig.14: Variation of the temperature θ with *S* for Pr=0.72, Sc=0.24, Gr=Gc=M=K=0.1, Sr=2, Df=0.03, n= γ =1.

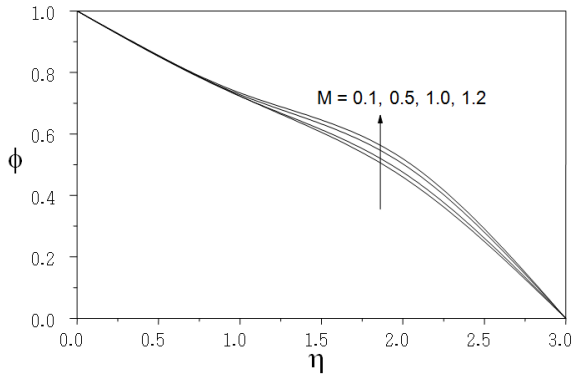

Fig.15: Variation of the concentration ϕ with M
for Pr=0.72,Sc=0.24,Gr=Gc=Ra=K=Ec=0.1, S=0, Sr=0.1, Df=0.03, n= γ =1.

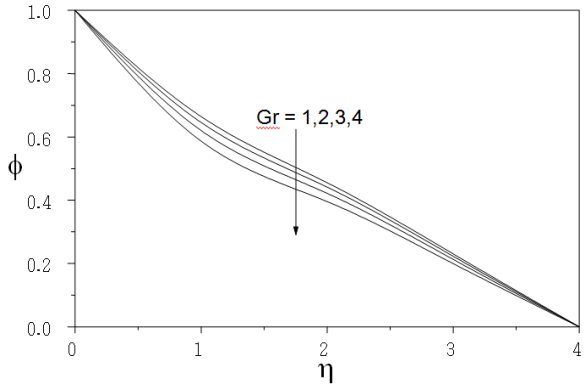

Fig.16: Variation of the concentration ϕ with Gr
for Pr=0.72, Sc=0.24, Gc=Ra=M=K=Ec=0.1, S=0, Sr=2, Df=0.03, γ =1.

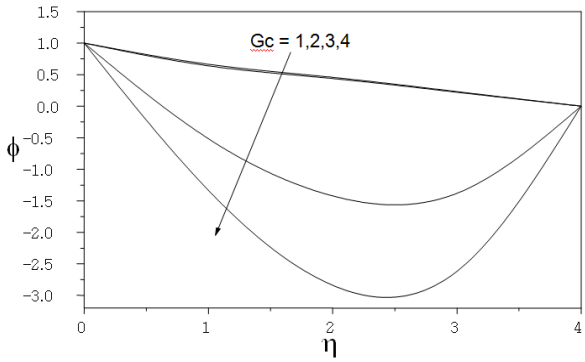

Fig.17: Variation of the concentration ϕ with Gc
for Pr=0.72, Sc=0.24, Gr=Ra=M=K=Ec=0.1, S=0, Sr=2, Df=0.03, n= γ =1.

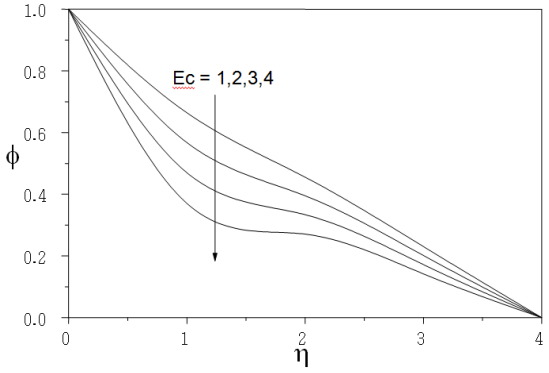

Fig.18: Variation of the concentration ϕ with Ec
for Pr=0.72, Sc=0.24, Gr=Gc=M=K=Ra=0.1, S=0, Sr=2, Df=0.03, n= γ =1.

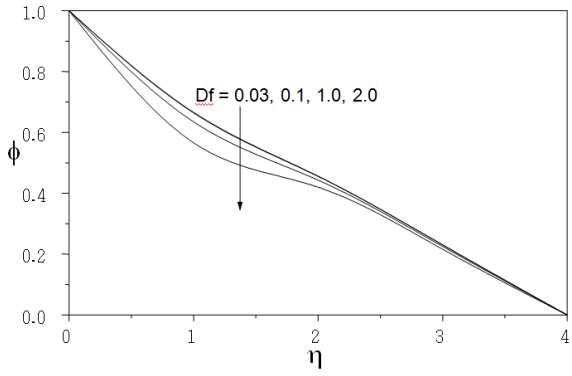

Fig.19: Variation of the concentration ϕ with Df
for Pr=0.72, Sc=0.24, Gr=Gc=M=K=Ra=Ec=0.1, S=0, Sr=2, n= γ =1.

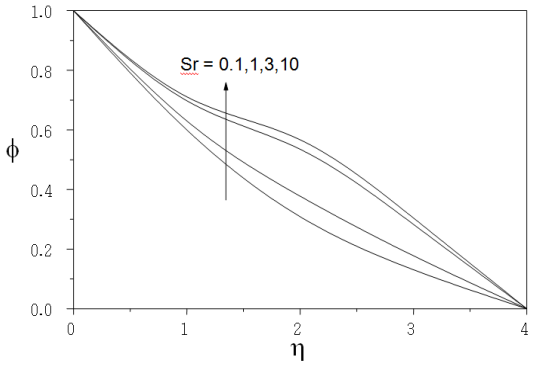

Fig.20: Variation of the concentration ϕ with Sr
for Pr=0.72, Sc=0.24, Gr=Gc=M=K=Ra=Ec=0.1, S=0, Df=0.03, γ =1.

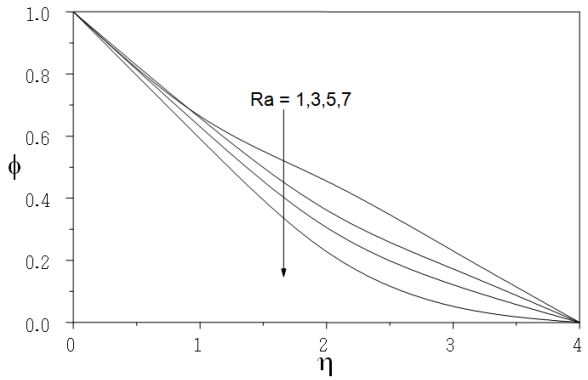

Fig.21: Variation of the concentration ϕ with Ra for Pr=0.72, Sc=0.24, Gr=Gc=M=K=Ec=0.1, S=0, , S=0, Sr=2, Df=0.03, γ =1

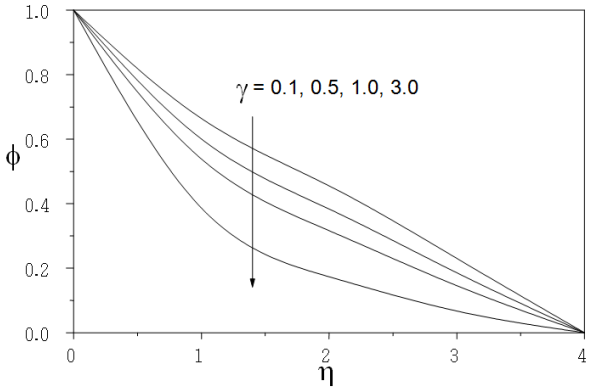

Fig.22: Variation of the concentration ϕ with γ for Pr=0.72, Sc=0.24, Gr=Gc=M=K=Ec=0.1, S=0, Sr=2, Df=0.03, n=1.

Table 1: Computation showing values of $f''(0)$, $-\theta'(0)$, $-\phi'(0)$ for different values of *S, K, Pr,* Gr, Gc, *M, Ra, Df, Sr, Ec,* γ and n

S	K	Pr	Gr	Gc	Sc	M	Ra	Df	Sr	γ	n	Ec	$-f''(0)$	$-\theta'(0)$	$-\phi'(0)$
-1	0.1	0.71	0.1	0.1	0.24	0.1	0.1	0.03	0.1	0.1	1	0.1	0.753561	1.26679	0.290138
0	0.1	0.71	0.1	0.1	0.24	0.1	0.1	0.03	0.1	0.1	1	0.1	0.816717	-0.125116	0.22532
1	0.1	0.71	0.1	0.1	0.24	0.1	0.1	0.03	0.1	0.1	1	0.1	0.925195	-2.31766	0.0723351
1	0.5	0.71	0.1	0.1	0.24	0.1	0.1	0.03	0.1	0.1	1	0.1	1.20702	-3.04967	-0.054538
1	1.0	0.7	1	0.1	0.24	0.1	0.1	0.03	0.1	0.1	1	0.1	1.52106	-4.64433	-0.348762
1	0.1	1	3	1.	0.24	0.1	0.1	0.03	0.1	0.1	1	0.1	0.960276	-2.98065	0.0357649
1	0.1	1.5	0.1	3	0.4	0.1	0.1	0.03	0.1	0.1	1	0.1	1.03128	-4.40631	-0.0240526
1	0.1	0.71	0.1	0.1	0.5	0.1	0.1	0.03	0.1	0.1	1	0.1	2.047369	-0.276801	0.456166
1	0.1	0.71	0.1	0.1	0.24	1	0.1	0.03	0.1	0.1	1	0.1	3.18748	-0.236112	0.48983
1	0.1	0.71	0.1	0.1	0.24	0.5	0.1	0.03	0.1	0.1	1	0.1	1.62724	-2.68494	0.00232268
1	0.1	0.71	0.1	0.1	0.24	0.1	1	0.03	0.1	0.1	1	0.1	2.97558	-3.07001	-0.0583945
1	0.1	0.71	0.1	0.1	0.24	0.1	3	1	0.1	0.1	1	0.1	0.998556	-3.41944	-0.24051
1	0.1	0.71	0.1	0.1	0.24	0.1	0.1	3	1	0.1	1	0.1	1.145	-5.73529	-0.939072
1	0.1	0.71	0.1	0.1	0.24	0.1	0.1	0.3	3	0.1	1	0.1	1.20702	-4.64433	-0.348762
1	0.1	0.71	0.1	0.1	0.24	0.1	0.1	0.3	0.1	3	1	0.1	1.52106	-3.04967	-0.654538
1	0.1	0.71	0.1	0.1	0.24	0.1	0.1	0.3	0.1	5	1	0.1	0.838642	-0.64966	0.194311
1	0.1	0.71	0.1	0.1	0.24	0.1	0.1	0.3	0.1	0.1	1	0.1	0.812023	-0.120945	0.229333
1	0.1	0.71	0.1	0.1	0.24	0.1	0.1	0.3	0.1	0.1	1	0.1	0.917329	-2.17562	0.0788323
1	0.1	0.71	0.1	0.1	0.24	0.1	0.1	0.3	0.1	0.1	1	0.1	0.898397	-1.85846	0.107117
1	0.1	0.71	0.1	0.1	0.24	0.1	0.1	0.3	0.1	0.1	1	0.1	0.854449	-1.34365	0.50274
1	0.1	0.71	0.1	0.1	0.24	0.1	0.1	0.3	0.1	0.1	1	01	0.808473	-0.739061	0.892133
1	0.1	0.71	0.1	0.1	0.24	0.1	0.1	0.3	0.1	0.1	1	0.1	0.837402	-1.17019	0.827273
1	0.1	0.71	0.1	0.1	0.24	0.1	0.1	0.3	0.1	0.1	1	01	0.81953	-0.953722	1.08915
1	0.1	0.71	0.1	0.1	0.24	0.1	0.1	0.3	0.1	0.1	1	0.1	1.51158	-13.7392	-1.54376
1	0.1	0.71	0.1	0.1	0.24	0.1	0.1	0.3	0.1	0.1	1	0.1	1.45492	-1.59041	0.499902
1	0.1	0.71	0.1	0.1	0.24	0.1	0.1	0.3	0.1	0.1	1	0.1	0.926107	-2.33043	0.0676897
1	0.1	0.71	0.1	0.1	0.24	0.1	0.1	0.3	0.1	0.1	1	0.1	0.926822	-2.3404	0.0640078

Table 2 Numerical values of $f''(0), -\theta'(0)$ and $\theta(0)$ at the plate for different values of S when Gr=1,Gc=0.5, Pr=1, Sc=0.5, M=0, Ra=0, K=0, Df=0, Sr=0, n=0 γ =0. Comparison of the present results with that of Olanrewaju and Gbadeyan [23]

S	Olanrewaju and Gbadeyan [23]			Present work		
	$f''(0)$	$-\theta'(0)$	$\theta(0)$	$f''(0)$	$-\theta'(0)$	$\theta(0)$
-1	1.844462	1.390856	0.463174	1.06329	1.56958	0.366434
0	1.999553	0.639244	0.478964	1.60566	0.171252	0.202751
1	2.134287	-0.073040	0.491749	2.08517	0.0110597	0.585355

REFERENCES

[1] A. Bejan, I. Dincer, S. Lorente, A.F. Miguel and A.H. Reis , Porous and Complex Flow Structures in Modern Technologies, Springer, New York, NY, 2004.

[2] Ingham D.B. and Pop I. (Eds.), Transport Phenomena in Porous Media, Vol. II, Pergamon, Oxford, UK, 1998.

[3] D.B Ingham and I. Pop (Eds.)., Transport Phenomena in Porous Media, Vol. III, Elsevier, Oxford, UK, 2005.

[4] K. Vafai, Handbook of Porous Media, Marcel Dekker, New York, NY, 2000.

[5] K. Vafai, Handbook of Porous Media, Second edition, Taylor and Francis, New York, NY, 2005.

[6] G. Singh, P.R. Sharma and A.J. Chamkha, Effect of Volumetric Heat Generation/Absorption on Mixed Convection Stagnation Point Flow on an Isothermal Vertical Plate in Porous Media, Int. J. Industrial Mathematics, vol.2(2), pp. 59-71, 2010.

[7] A. Postelnicu, E. Magyari and I. Pop, Effect of a Uniform Horizontal through Flow on the Darcy Free Convection over a Permeable Vertical Plate with Volumetric Heat Generation, Transport in Porous Media, vol.80, pp.101-115, 2009.

[8] K. Vajravelu and A. Hadjinicolaou, Heat Transfer in Viscous Fluid over a Stretching Sheet with Viscous Dissipation and Internal Heat Generation, International Communication in Heat and Mass Transfer, vol.20, pp.417-430, 1993.

[9] K. Vajravelu and J. Nayfeh, Hydro magnetic Convection at a Cone and a Wedge, International Communication in Heat and Mass Transfer, vol.19, pp.701-710,1992.

[10] S. Shateyi, S. Motsa, and P. Sibanda, The Effects of Thermal Radiation, Hall Currents, Soret, and Dufour on MHD flow by Mixed Convection over a Vertical Surface in Porous Media, Mathematical Problems in Engineering, Article ID 627475. Doi:10.1155/2010/627475, 2010.

[11] R. S. R. Gorla and I. Pop, Conjugate Heat Transfer with Radiation from a Vertical Circular Pin in Non-Newtonian Ambient Medium, Warme Stoffubertr, vol. 28, pp.11-15, 1993.

[12] A.A. Mohammadein and M.F. El-Amin, Thermal Dispersion Radiation Effects on Non- Darcy Natural Convection in a Fluid Saturated Porous Medium, Transport Porous Media, vol.40, pp.153- 163, 2000.

[13] H. Duwairi and R. M. Duwairi, Thermal Radiation Effects on MHD-Rayleigh Flow with Constant Surface Heat Flux, Heat Mass Transfer, vol.41, pp.51-57, 2004.

[14] S.R .Pop, T. Grosan and I. Pop, Radiation Effects on the Flow Near the Stagnation Point of a Stretching Sheet, Tech. Mech., vol.25, pp.100-106, 2004.

[15] T. Hayat, M. Mustafa and I. Pop, Heat and Mass Transfer for Soret and Dufour Effect on Mixed Convection Boundary Layer Flow over a Stretching Vertical Surface in a Porous Medium filled with a Visco-elastic Fluid, Commun. Nonlinear Sci Numer Simulat, vol.15, pp.1183-1196, 2010.

[16] Z. Abbas, Y. Wang, T. Hayat and M. Oberlack (In Press), Mixed Convection in the Stagnation-Point flow of a Maxwell Fluid Towards a Vertical Stretching Surface, Nonlinear Analysis, Real World Applications.

[17] B. Gebhart and J. Mollendorf, Viscous dissipation in external natural convection flows, J. Fluid. Mech., vol. 38, pp. 97-107, 1969.

[18] V.M. Soundalgekar, Viscous dissipation effects on unsteady free convective flow past an infinite, vertical porous plate with constant suction, Int. J. Heat Mass Transfer, vol.15, pp. 1253-1261, 1972.

[19] C. Israel-Cookey, A. Ogulu and V.B. Omubo-Pepple, Influence of viscous dissipation on unsteady MHD free-convection flow past an infinite heated vertical plate in porous medium with time-dependent suction, Int. J. Heat Mass transfer, vol. 46, pp. 2305-2311, 2003.

[20] V. Ramachandra Prasad and N. Bhaskar Reddy, Radiation and mass transfer effects on an unsteady MHD free convection flow past a heated vertical plate in a porous medium with viscous dissipation, Theoretical. Applied Mechanics, vol. 34, No.2, pp.135-160, 2007.

[21] M. Gnaneshwara Reddy and N. Bhaskar Reddy, Radiation and mass transfer effects on an unsteady MHD free convection flow past a heated vertical porous plate with viscous dissipation, Int. J. of Appl. Math and Mech,vol.6, No.6, pp.96-110, 2010.

[22] S. Suneetha and N. Bhaskar Reddy, Radiation and Darcy effects on unsteady MHD heat and mass transfer flow of a chemically reacting fluid past an impulsively started vertical plate with heat generation, Int. J. of Appl. Math and Mech.,vol.**7** (7), pp.1-19, 2011.

[23] P.O Olanrewaju and J.A Gbadeyan, Effects of Soret, Dufour, Chemical reaction,Thermal Radiation and Volumetric Heat Generation/absorption on mixed convection stagnation point flow on an isothermal vertical plate in porous media. The specific journal of science and technology, vol.12, pp.234-245, 2011.